Band Structure of CaCd and CaTl and the Knight Shift of ^{113}Cd- and ^{205}Tl-NMR in the System $CaCd_{1-x}Tl_x$

P. C. Schmidt and Alarich Weiss

Physikalische Chemie III, Technische Hochschule Darmstadt, Germany

(Z. Naturforsch. **29 a**, 477–487 [1974]; received 20 December 1973)

The energy bands of ordered CaCd and CaTl have been calculated by the nonrelativistic augmented plane wave (APW) method. The electron structure in the system $CaCd_{1-x}Tl_x$ is deduced from these calculations by using the rigid band model for the phases with $0<x<1$. The band structures of CaCd and CaTl are similar to the valence bands of other phases of the CsCl-type. From the energy eigenvalues the electronic density of states curve, the partial densities of states curves, and the Fermi energy have been obtained. For states near the Fermi surface the spin density at the position of the Cd- and Tl-nuclei has been determined.

The Knight shift K_s of the ^{113}Cd-NMR and the ^{205}Tl-NMR in the system $CaCd_{1-x}Tl_x$ has been calculated as a function of x. The slope of the curve $K_s(x)$ for the Cd-NMR is equal for experimental and theoretical results. The absolute value of the calculated Knight shift is about a factor of 1.4 too small. Only the direct term to the Knight shift has been calculated. Relativistic effects have been included by a scale factor. It has not been possible to explain the shape of the function $K_s(x)$ for the Tl-NMR, since a full relativistic APW calculation is necessary for CaTl.

Introduction

In the course of investigations of ternary intermetallic compounds the quasibinary system $CaCd_{1-x}Tl_x$ has been studied by X-ray diffraction. The alloys of this system form homogeneous solid solutions for all concentrations x: $0 \leqq x \leqq 1$. They crystallize with the space group O_h^1-Pm3m and one formula unit per unit cell (CsCl-type). Furthermore, concentration dependent nuclear magnetic resonance (NMR) measurements were carried out on these alloys using ^{113}Cd- and ^{205}Tl-nuclei as NMR probes. It was found that the Knight shift K_s of the Cd- and Tl-NMR varies continuously as a function of x. However, the functions $K_s = f(x)$ for the Cd- and Tl-NMR shifts have different slopes [1]. The purpose of this paper is a theoretical approach to the interpretation of the experimental results.

Since the Knight shift K_s depends on the wave function density at the nuclei and the density of states at the Fermi energy, band structure calculations for an interpretation of $K_s = f(x)$ are desirable. The band structure calculations for the boundary phases CaCd and CaTl have been done using the non-relativistic augmented plane wave (APW) method [2, 3]. From the calculated energy eigenvalues the Fermi energies and the density of states have been determined. Finally, the Knight shift is analysed. For the phases CaCd and CaTl the relativistic contribution to K_s is estimated. To analyse K_s along the quasibinary section $CaCd_{1-x}Tl_x$, $0 \leqq x \leqq 1$, the rigid band model [4] is used.

The band structures of several intermetallic compounds of the CsCl-type have already been studied using the APW method [5–8]. The results of these calculations were compared with optical data, with measurements of the specific heats of the electrons, and with the de Haas-van Alphen experiments. To calculate the Knight shift [9–11], mostly the orthogonalized plane wave method is used in the literature. The Knight shift in alloys was studied theoretically as a function of the mixing proportion by applying the rigid band model [12, 13] or the theory of the Friedel oscillations [14–16].

Reprint requests to: Prof. Dr. A. Weiss, Physikalische Chemie III, Technische Hochschule, *D-6100 Darmstadt*, Germany.

The Band Structure of CaCd and CaTl in the Non-Relativistic APW Approximation

1. Potential and APW Wave Functions

For the calculation of energy states in solids by the APW method, the real lattice potential for the electrons in the crystals is approximated by the so-called muffin-tin potential. In a model assumption the crystal is separated into two regions (Figure 1). In region I, spherical symmetric potentials are defined around the sites of the atomic nuclei. These atomic spheres do not overlap. The potential between these spheres in region II is taken to be a

constant one (APW constant). Because of the high symmetry of the crystals and the flat real potential between the spheres, the muffin-tin potentials is a good approximation for metals and alloys. Region I is chosen as large as possible and, therefore, the atomic spheres touch each other in the direction of nearest neighbours. The radii of the atomic spheres of region I are called APW radii R_ν.

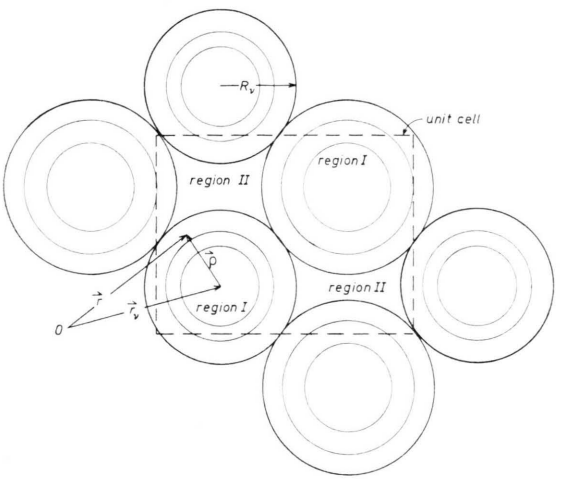

Fig. 1. Muffin-tin potential in the (111) plane for the cubic primitive structure. In region I the potentials are spherically symmetric around the positions of the nuclei $\boldsymbol{r}_\nu$. In region II the potential is a constant one.

The muffin-tin potentials have been obtained by a) the coulomb potentials due to the nuclei and the electrons of the central atom, b) by the spherically symmetric part of the coulomb potentials due to the 14 nearest neighbours in the CsCl structure, and c) by the exchange potentials. The exchange potentials are calculated in the free electron exchange approximation of Slater [17] (Hartree-Fock-Slater approximation).

If the zero of the energy scale is shifted to the APW constant, the constant potential in region II is zero.

In the muffin-tin approximation, the wave functions in region II are plane waves

$$\varphi_{i\,\mathrm{II}}(\boldsymbol{r}) = \exp\{i\,\boldsymbol{k}_i\,\boldsymbol{r}\}\,, \tag{1}$$

$$\boldsymbol{k}_i = \boldsymbol{k} + \boldsymbol{g}_i\,. \tag{2}$$

$\boldsymbol{k}$ is the wave vector of the first Brillouin zone, $\boldsymbol{g}_i$ is a reciprocal lattice vector. Inside the sphere ν the wave functions can be expanded in spherical harmonics Y_{lm}:

$$\varphi_{i\mathrm{I}}(\boldsymbol{r}) = \sum_{l=0}^{\infty}\sum_{m=-l}^{l} a_{\nu m}^{(i)} Y_{lm}(\hat{\varrho})\,u_l(\varrho, E)\,. \tag{3}$$

$$\boldsymbol{\varrho} = \boldsymbol{r} - \boldsymbol{r}_\nu\,, \tag{4}$$

$$\hat{\varrho} = \boldsymbol{\varrho}/\varrho\,. \tag{5}$$

The radial wave function $u_l(\varrho, E)$ is the solution of the radial Schrödinger equation in the muffin-tin potential with the angular momentum l. E is the energy of the state $\boldsymbol{k}$ being investigated. In the APW scheme proposed by Slater [18], the function

$$\varphi_i = \begin{cases} \varphi_{i\mathrm{I}} & \text{in region I;} \\ \varphi_{i\mathrm{II}} & \text{in region II} \end{cases} \tag{6}$$

is made continuous at the boundary of region I and II by a proper choice of the coefficients $a_{lm}^{(i)}$. Expanding the plane wave also in spherical harmonics and in spherical Bessel-functions j_l, it follows:

$$a_{lm}^{(i)} = 4\,\pi \exp\{i\,\boldsymbol{k}_i\,\boldsymbol{r}_\nu\}\; i^l\, j_e(k_i\,R_\nu)\, Y_{lm}^*(\hat{\boldsymbol{k}}_i)/u_e(R_\nu, \mathrm{E})\,. \tag{7}$$

The continuous function φ_i is called an augmented plane wave and is shown in Figure 2. The wave

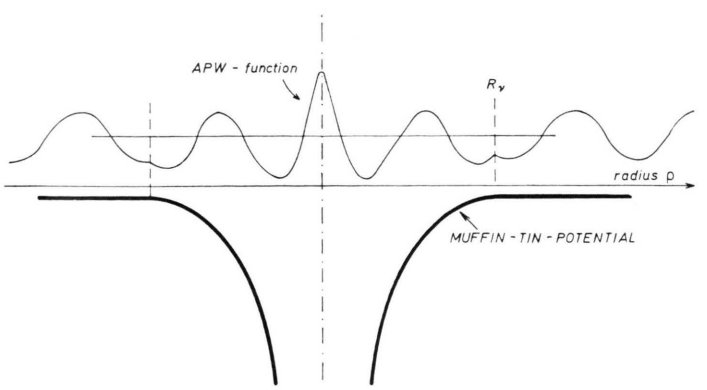

Fig. 2. Muffin-tin potential and APW function.

function $\psi_{\boldsymbol{k}}(\boldsymbol{r})$ of an electron in the crystal with wave vektor $\boldsymbol{k}$ is regarded as an expansion of the APW functions:

$$\psi_{\boldsymbol{k}}(\boldsymbol{r}) = (1/N_{\boldsymbol{k}}) \sum_i v_i \varphi_i(\boldsymbol{r}) \,. \tag{8}$$

The coefficients $v_i = v(\boldsymbol{k}_i)$ are determined by a variation procedure. $N_{\boldsymbol{k}}$ is the normalisation constant and the summation is taken over the reciprocal lattice.

Besides the energy eigenvalues, the charge outside and inside the APW spheres can be calculated [19]. To do so, the square of the wave function is integrated over region II and I. For a crystal with a cubic primitive unit cell, it follows [3]

$$Q^{\boldsymbol{k}}_{\text{out}} \frac{\Omega}{N_{\boldsymbol{k}}} \sum v_i v_j A_{ij} \,, \tag{9}$$

and

$$Q^{\boldsymbol{k}}_{in} = \sum_{\nu=1}^{2} \sum_l Q^{\boldsymbol{k}}_{\nu l} \,, \tag{10}$$

with

$$Q^{\boldsymbol{k}}_{\nu l} = \frac{\Omega}{N_{\boldsymbol{k}}} \sum_{ij} v_i v_j C^{(\nu)}_{ijl} I_{\nu l} \,, \tag{11}$$

respectively.

A_{ij}, $C^{(\nu)}_{ijl}$ and $I_{\nu l}$ are abbreviations for the following expressions

$$A_{ij} = \delta_{ij} - \sum_{\nu=1}^{2} \frac{4\pi R_\nu^2}{\Omega} \exp\{i \boldsymbol{k}_{ij} \boldsymbol{r}_\nu\} \, j_1(k_{ij} R_\nu) \, k_{ij}^{-1}, \tag{11 a}$$

$$C^{(\nu)}_{ijl} = \frac{4\pi R_\nu^2}{\Omega} (2l+1) j_l(k_j R_\nu) P_l(\hat{k}_i \hat{k}_j) \cdot \exp\{i \boldsymbol{k}_{ij} \boldsymbol{r}_\nu\} \,, \tag{11 b}$$

$$I_{\nu l} = \int_0^{R_\nu} \left[\frac{\varrho \, u_l(\varrho, E)}{R_\nu \, u_l(R_\nu, E)} \right]^2 \mathrm{d}\varrho \,, \tag{11 c}$$

$$\boldsymbol{k}_{ij} = \boldsymbol{k}_i - \boldsymbol{k}_j .$$

Ω is the volume of the unit cell, δ_{ij} is the Kronecker symbol and P_l is the Legendre polynom.

If the normalisation constant $N_{\boldsymbol{k}}$ is chosen that

$$Q^{\boldsymbol{k}}_{\text{out}} + Q^{\boldsymbol{k}}_{\text{in}} = 1 \,, \tag{12}$$

we can interprete the APW charges $Q^{\boldsymbol{k}}_{\text{in}}$ and $Q^{\boldsymbol{k}}_{\text{out}}$ in units of the electron charge as fraction of the charge of the state $\psi_{\boldsymbol{k}}$ inside and outside the atomic spheres. Inside the sphere $Q^{\boldsymbol{k}}_{\nu l}$ represents the fractional charge associated with the angular momentum l. It is shown below that the Knight shift is approximately a function of the charge $Q_{\nu 0}$.

2. Computational Details for the APW Calculations

Both phases, CaCd and CaTl, belong to the CsCl-type. The first Brillouin zone is shown in Figure 3.

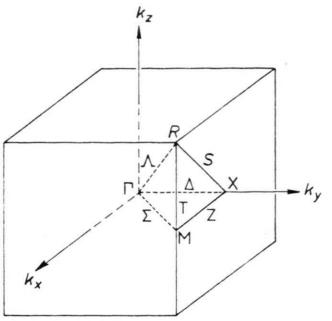

Fig. 3. Brillouin zone for the CsCl structure.

For the free atoms with the electron configuration of Table 1, the muffin-tin potential was constructed

Table 1. Values of parameters involved in the APW calculation for CaCd and CaTl.

Alloy	CaCd	CaTl
Structure type	CsCl	CsCl
Lattice parameter [1] a	7.2521 a_0	7.2793 a_0
Volume of the unit cell Ω	381.41 a_0^3	385.72 a_0^3
Electron configuration	Ca: $3p^6\,4s^2$	Ca: $3p^6\,4s^2$
	Cd: $4d^{10}\,5s^2$	Tl: $5d^{10}\,6s^2\,6p^1$
APW constant	−0.8635 Ry	−0.9202 Ry
APW sphere radii R_ν	Ca: 3.158 a_0	Ca: 3.004 a_0
	Cd: 3.004 a_0	Tl: 3.158 a_0

[1] $a_0 = 0.5292$ Å is the Bohr radius.

using the self-consistent Hartree-Fock-Slater wave functions of Herman and Skillman [20]. The radii of the APW spheres and the constant potential between the spheres are given by the intersection of the single potentials in the [111]-direction. In Table 1, the values of the different parameters involved in the APW calculation are given.

The summation of Eq. (8) is evaluated including all wave vektors $\boldsymbol{k}_i$ satisfying $k_i \leqq k_{\max}$, where $k_{\max}$ is given by a condition proposed by Switendick [3]

$$k_{\max} R_s = 6 \,, \tag{13}$$

where R_s is the smaller APW radius of the different atomic spheres. For a general $\boldsymbol{k}$ point the condition (13) implicates 50 – 60 basis functions. Instead of Eq. (13), the weaker condition $k_{\max} R_s = 5$ changes the energy values up to 0.005 Ry for states at the Fermi surface.

In the summation over l in Eq. (3) all values of l up to $l_{\max} = 5$ were included. For states near the

Fermi energy, an upper boundary of $l_{\max} = 12$ changes the energy values less than 0.001 Ry. The APW charges $Q_{vl}^{\boldsymbol{k}}$ vary under the same conditions less than 4%. This variation can be neglected for the analysis of the Knight shift data.

3. Bands of CaCd and CaTl

The APW calculations show that in CaCd and CaTl the bands of the core electrons and the valence electrons do not overlap. Therefore, in the following only the valence and conduction bands are considered.

The eigenvalues of these bands have been obtained for 35 non-equivalent wave vectors $\boldsymbol{k}$ in the reduced zone, corresponding to 512 $\boldsymbol{k}$ points in the full Brillouin zone. In CaCd six eigenvalues were determined for each $\boldsymbol{k}$. Assuming that the conduction bands of CaCd and CaTl are very similar in the non-relativistic APW calculation, we have determined only four bands in CaTl.

In Tables A1 and A2, the energy values and the multiplicities $M(\boldsymbol{k}_t)$ are given for the 35 $\boldsymbol{k}$ vectors $\boldsymbol{k}_t$. $M(\boldsymbol{k}_t)$ is the number of states having the same energy eigenvalue as $\boldsymbol{k}_t$. In Figs. 4 and 5 the bands are shown along the principal symmetry lines (see Figure 3). Throughout this work the APW scale has been used. The APW constants given in Table 1 have to be added to all given energy values.

The calculated band structures of CaCd and CaTl are qualitatively very similar. Only the points M_5' and R_2' are lowered in CaTl. Because a relativistic APW calculation is necessary for CaTl, the following discussion is restricted to the bands of CaCd.

For a detailed discussion of the band shapes it is useful to know the APW charges $Q_{vl}^{\boldsymbol{k}}$. If $Q_{\mathrm{Cd},1}^{\boldsymbol{k}}$ is much greater for one band than the other $Q_{vl}^{\boldsymbol{k}}$ in Eq.

Table A 1. Energy bands of CaCd in the non-relativistic APW approximation. The wave vectors $\boldsymbol{k}_t$ are given in units of $\pi/4\,a$. $M(\boldsymbol{k}_t)$ is the multiplicity of the state $\boldsymbol{k}_t$. To all energy values given in Ry the APW constant of −0.8635 Ry has to be added.

$\boldsymbol{k}_t$	$M(\boldsymbol{k}_t)$	1st band	2nd band	3rd band	4th band	5th band	6th band
0 0 0	1	−0.0502	0.3830	0.3830	0.5072	0.5072	0.5072
0 1 0	6	−0.0374	0.3789	0.3859	0.5020	0.5020	0.5154
0 2 0	6	0.0003	0.3384	0.3918	0.4740	0.4740	0.5163
0 3 0	6	0.0607	0.2526	0.3974	0.4520	0.4520	0.5166
0 4 0	3	0.1191	0.1803	0.3981	0.4440	0.4440	0.5144
1 1 0	12	−0.0248	0.3795	0.3832	0.4809	0.4950	0.5109
1 2 0	24	0.0123	0.3459	0.3904	0.4536	0.4747	0.5100
1 3 0	24	0.0712	0.2623	0.3999	0.4420	0.4558	0.5100
1 4 0	12	0.1258	0.1947	0.4029	0.4347	0.4492	0.5104
2 2 0	12	0.0474	0.3575	0.3678	0.4365	0.4742	0.4985
2 3 0	24	0.1013	0.2893	0.3872	0.4292	0.4652	0.4961
2 4 0	12	0.1455	0.2356	0.4085	0.4142	0.4613	0.4973
3 3 0	12	0.1447	0.3169	0.3532	0.4244	0.4772	0.4857
3 4 0	12	0.1735	0.2959	0.3683	0.4117	0.4750	0.4833
4 4 0	3	0.1906	0.3460	0.3460	0.3852	0.4800	0.4800
1 1 1	8	−0.0124	0.3830	0.3830	0.4696	0.4940	0.4940
1 2 1	24	0.0241	0.3520	0.3907	0.4542	0.4624	0.4987
1 3 1	24	0.0814	0.2720	0.4012	0.4366	0.4582	0.5013
1 4 1	12	0.1327	0.2083	0.4118	0.4225	0.4594	0.5027
2 2 1	24	0.0583	0.3660	0.3691	0.4409	0.4607	0.4832
2 3 1	48	0.1110	0.2984	0.3857	0.4328	0.4705	0.4860
2 4 1	24	0.1531	0.2467	0.3951	0.4242	0.4777	0.4864
3 3 1	24	0.1535	0.3247	0.3481	0.4285	0.4774	0.4865
3 4 1	24	0.1823	0.3004	0.3592	0.4192	0.4894	0.4909
4 4 1	6	0.1996	0.3380	0.3380	0.4006	0.4980	0.4980
2 2 2	8	0.0900	0.3720	0.3720	0.4352	0.4600	0.4600
2 3 2	24	0.1384	0.3192	0.3721	0.4488	0.4602	0.4820
2 4 2	12	0.1755	0.2752	0.3720	0.4522	0.4743	0.5068
3 3 2	24	0.1789	0.3359	0.3374	0.4509	0.4900	0.4900
3 4 2	24	0.2078	0.3076	0.3417	0.4505	0.4967	0.5339
4 4 2	6	0.2284	0.3220	0.3220	0.4457	0.5450	0.5682
3 3 3	8	0.2175	0.3270	0.3270	0.4985	0.4985	0.5080
3 4 3	12	0.2454	0.3088	0.3231	0.5005	0.5098	0.5244
4 4 3	6	0.2730	0.3080	0.3080	0.4900	0.5071	0.5460
4 4 4	1	0.3012	0.3012	0.3012	0.4431	0.4431	0.4431

Table A 2. Energy bands of CaTl in the non-relativistic APW approximation. The wave vectors $\boldsymbol{k}_t$ are given in units of $\pi/4\,a$. $M(\boldsymbol{k}_t)$ is the multiplicity of the state $\boldsymbol{k}_t$. To all energy values given in Ry the APW constant of -0.9202 Ry has to be added.

$\boldsymbol{k}_t$	$M(\boldsymbol{k}_t)$	1st band	2nd band	3rd band	4th band
0 0 0	1	−0.1089	0.4170	0.4170	0.5605
0 1 0	6	−0.0965	0.4011	0.4196	0.5280
0 2 0	6	−0.0602	0.3272	0.4289	0.5020
0 3 0	6	−0.0044	0.2246	0.4354	0.4780
0 4 0	3	0.0391	0.1623	0.4355	0.4690
1 1 0	12	−0.0843	0.4010	0.4103	0.5048
1 2 0	24	−0.0487	0.3354	0.4170	0.4804
1 3 0	24	0.0057	0.2354	0.4303	0.4632
1 4 0	12	0.0468	0.1761	0.4436	0.4522
2 2 0	12	−0.0153	0.3528	0.3612	0.4692
2 3 0	24	0.0343	0.2662	0.3859	0.4605
2 4 0	12	0.0693	0.2150	0.4028	0.4488
3 3 0	12	0.0751	0.2991	0.3239	0.4510
3 4 0	12	0.1009	0.2709	0.3409	0.4360
4 4 0	3	0.1195	0.3090	0.3090	0.4115
1 1 1	8	−0.0724	0.4050	0.4050	0.4824
1 2 1	24	−0.0375	0.3431	0.4136	0.4711
1 3 1	24	0.0156	0.2461	0.4285	0.4663
1 4 1	12	0.0548	0.1891	0.4398	0.4486
2 2 1	24	−0.0047	0.3629	0.3632	0.4648
2 3 1	48	0.0440	0.2757	0.3857	0.4674
2 4 1	24	0.0778	0.2253	0.3958	0.4584
3 3 1	24	0.0848	0.3081	0.3228	0.4589
3 4 1	24	0.1110	0.2758	0.3383	0.4471
4 4 1	6	0.1309	0.3070	0.3070	0.4274
2 2 2	8	0.0263	0.3680	0.3680	0.4321
2 3 2	24	0.0720	0.2988	0.3722	0.4692
2 4 2	12	0.1035	0.2530	0.3739	0.4850
3 3 2	24	0.1131	0.3204	0.3233	0.4717
3 4 2	24	0.1408	0.2860	0.3310	0.4822
4 4 2	6	0.1650	0.3020	0.3020	0.4751
3 3 3	8	0.1562	0.3170	0.3170	0.4573
3 4 3	12	0.1867	0.2939	0.3148	0.4467
4 4 3	6	0.2224	0.2950	0.2950	0.4071
4 4 4	1	0.2942	0.2942	0.2942	0.3154

(10), we shall call this band a p-like band of Cd. If two or more $Q_{vl}^{\boldsymbol{k}}$ values are of the same order, hybrid bands are obtained. Often electrons belonging to atomic energy levels with the angular momentum l form l-like bands in metals and alloys. In CaCd the lowest band in the energy range $E(\Gamma_1)$ to $E(X_4')$ is a s-like band of Cd. The band is similar to the band of the free electron gas. Above $E(X_4')$ up to $E(R_{25}')$ this s-like band is hybridized with a p-like band of Cd and a d-like band of Ca. Above $E(R_{25}')$, CaCd has five d-like bands of Ca hybridized with s-like and p-like bands of Cd. Therefore, a broad valence band between -0.05 Ry and 0.3 Ry results. Above this value five narrow bands in the range $0.3-0.5$ Ry for CaCd appear. An exception are the states around the point X_1. Near this point the second band is far below 0.3 Ry. These are the only states with a measurable s portion $Q_{\mathrm{Ca},0}^{\boldsymbol{k}}$ of Ca. The non-relativistic calculations in CaTl yield similar charge distributions.

Broad valence bands and narrow d-like bands are also characteristic for other intermetallic compounds with CsCl structure, such as β'-CuZn [5], β'-NiAl [6], β'-PdIn [7], YCu [8], and YZn [8], although the width and the degree of hybridization of the d-like bands are different for the individual alloys. In contrast to CaCd and CaTl, in all the phases cited above the d-like bands can be assigned to the d levels of the different elements, e.g. in β'-PdIn the s-like valence bands are hybridized with the 4d bands of Pd [7]. The mathematical reason for the analogy of Ca and a transition element in relation to the band structure is the similar shape of the logarithmic derivatives of the radial wave function $u_l(R_\nu, E)/u_l'(R_\nu, E)$ with $l = 0.1$ and 2 as a function of E.

Density of States and Fermi Energy

The density of states $n(E)$ is defined as the number of electrons (or states with spin degeneration) per unit volume of the metal in the energy range ΔE around E per unit range of energy. Histograms can be constructed for $n(E)$ using the energy values of the states given in Tables A 1 and A 2 [21, 22].

Because of the limited number of states $\boldsymbol{k}_t$ being considered, the shape of the histograms depends on the energy intervals ΔE used [21, 22]. For calculations done in this work we could not choose ΔE smaller than 0.03 Ry. It is averaged over six different density of states histograms. For convenience, in Figs. 6 and 7 the densities of states $N(E)$ per unit cell and per Ry are shown,

$$N(E) = \Omega\, n(E)\,. \tag{14}$$

The density of states for CaCd has two broad peaks at about 0.0 and 0.15 Ry which are mainly due to the 4 s band of Cd. The third peak at about 0.36 Ry belongs predominantly to the d-like bands of Ca hybridized with the p-like bands of Cd. As the band structure, the shape of the density of states for CaCd is very similar to the corresponding curve for YZn. The density of states for CaTl has a broad peak at about 0.05 Ry due to the 5 s band of Tl. The second peak at about 0.3 Ry and the ascent at 0.43 Ry belong to the d-like bands of Ca hybridized with the p-like bands of Tl.

Besides the total density of states $N(E)$, partial densities of states $N_{vl}(E)$ were calculated. These

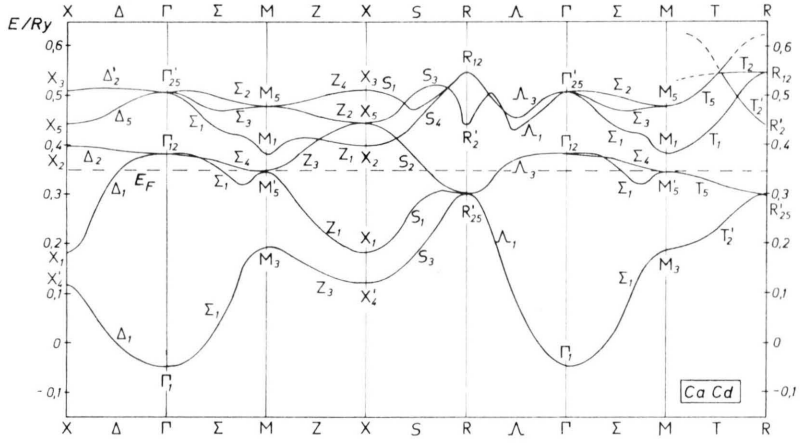

Fig. 4. Energy bands of CaCd for the directions in $\boldsymbol{k}$ space given in Figure 3.

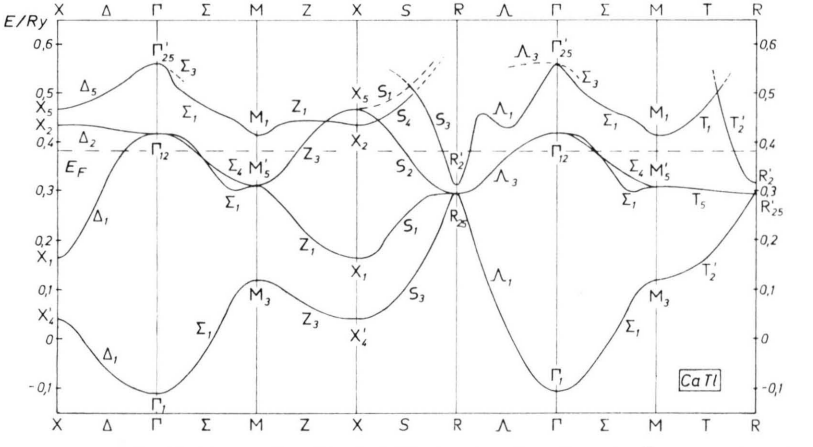

Fig. 5. Energy bands of CaTl for the directions in $\boldsymbol{k}$ space given in Figure 3.

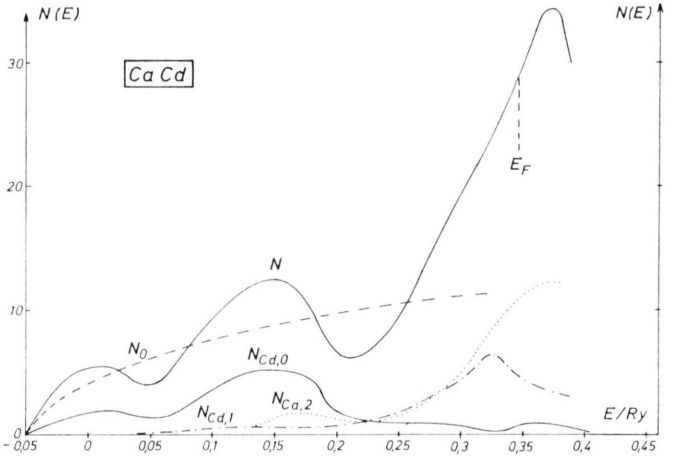

Fig. 6. Density of states of CaCd given in electrons per unit cell and per Ry. N_0 is the density of states calculated from the free electron model. N is the total density of states in the APW approximation. $N_{\nu,l}$ are partial densities of states, which are a function of the atomic sphere ν and the angular momentum l.

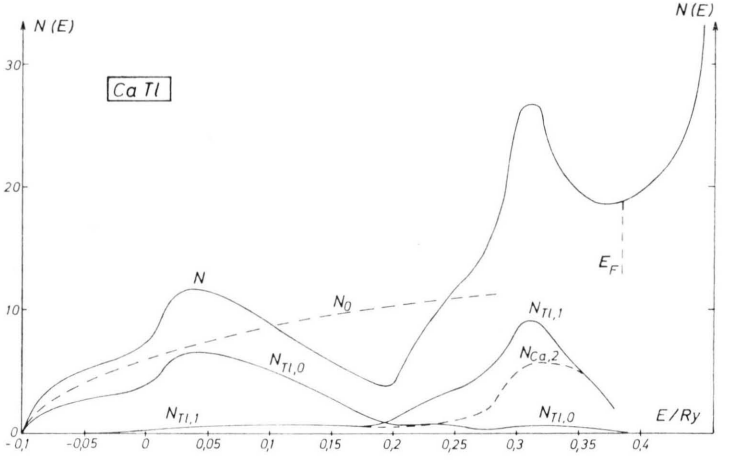

Fig. 7. Density of states of CaTl given in electrons per unit cell and per Ry. N_0 is the density of states calculated from the free electron model. N is the total density of states in the APW approximation. $N_{\nu,l}$ are partial densities of states, which are a function of the atomic sphere ν and the angular momentum l.

densities depend on the angular momentum l and the atomic sphere ν. The total density $N(E)$ is the sum of the partial densities of states,

$$N(E) = \sum_{\nu l} N_{\nu l}(E) + N_{\text{out}} . \tag{15}$$

The main partial densities of states for CaCd and CaTl are shown in Figs. 6 and 7. Except N_{out}, all other partial densities of states are small compared to the plotted ones. The first two peaks of the total density of states of CaCd correspond to the maximum of the partial density of states $N_{\text{Cd},0}$ and the third peak of $N(E)$ corresponds to the maxima of $N_{\text{Cd},1}$ and $N_{\text{Ca},2}$. In CaTl the partial densities have a similar shape as in CaCd, but in CaTl the maxima of the partial densities $N_{\text{Tl},1}$ and $N_{\text{Ca},2}$ are lying at the same energy value, whereas in CaCd the maxima of $N_{\text{Cd},1}$ and $N_{\text{Ca},2}$ belong to different energy values.

To calculate the Fermi energy E_{F}, $N(E)$ is integrated over E from the lowest energy value $E(\Gamma_1)$ up to the total number of electrons per unit cell z,

$$\int_{E(\Gamma_1)}^{E_{\text{F}}} N(E)\,\mathrm{d}E = z . \tag{16}$$

In our approximation we count the number of states given in Tables A1 or A2, respectively, from the lowest energy value up to the boundary z,

$$\frac{2}{512} \sum_{E_t \leqq E_{\text{F}}} M(\boldsymbol{k}[E_t]) = z . \tag{17}$$

For CaCd, z is equal 4 and the energy value of $E_{\text{F}} = 0.348$ Ry is reached at the point $k_t = \pi(3,3,1)/(4a)$ in the third band, where $M[\boldsymbol{k}_t(0.348)]$ is 24. For CaCd the Fermi energy lies in a range with large p partial density of states of Cd and large d partial density of Ca and small s partial density of Cd.

Knight Shift

1. Calculation of the Knight Shift

For the theoretical discussion of the NMR measurements, we assume that the Knight shift K_{s} is given by the hyperfine contact term [23]

$$K_{\text{s}}^{\text{d}} = \frac{8\pi}{3} \chi_{\text{p}} \Omega \langle |\psi_{\boldsymbol{k}}(\boldsymbol{r}_\nu)|^2 \rangle_{\text{F}} . \tag{18}$$

although K_{s}^{d} is only the direct contribution to K_{s}. χ_{p} is the Pauli spin susceptibility per unit volume. $\langle |\psi_{\boldsymbol{k}}(\boldsymbol{r}_\nu)|^2 \rangle_{\text{F}}$ is the averaged direct spin density at the nuclear site $\boldsymbol{r}_\nu$ due to the conduction electrons at the Fermi surface.

To calculate the square of the APW wave function, one starts with a spherical averaged radial charge density $\sigma_\nu^{\boldsymbol{k}}$. By integrating $r^2 \psi \psi^*$ over solid angles within each of the APW spheres [3]

$$\sigma_\nu^{\boldsymbol{k}}(\varrho) = \frac{\Omega}{N_{\boldsymbol{k}}} \sum_l \sum_{ij} v_i v_j C_{ijl}^{(\nu)} \left[\frac{\varrho\, u_l(\varrho, E)}{R_\nu\, u_l(R_\nu, E)} \right]^2 \tag{19}$$

follows.

The square of the wave function at the nuclear position is given by

$$|\psi_{\boldsymbol{k}}(\boldsymbol{r}_\nu)|^2 = \lim_{\varrho \to 0} \frac{\sigma_\nu^{\boldsymbol{k}}(\varrho)}{4\pi\varrho^2} . \tag{20}$$

With

$$G_{\nu l}^{\boldsymbol{k}} = \lim_{\varrho \to 0} \frac{1}{4\pi} \left[\frac{u_l(\varrho, E)}{R_\nu\, u_l(R_\nu, E)} \right]^2 \tag{21}$$

one gets:

$$|\psi_{\boldsymbol{k}}(\boldsymbol{r}_\nu)|^2 = Q_{\nu 0}^{\boldsymbol{k}} G_{\nu 0}^{\boldsymbol{k}} / I_{\nu 0}^{\boldsymbol{k}}, \tag{22}$$

for $G_{\nu l} = 0$ for $l \neq 0$. Only the s part of the wave function is unequal zero at the nuclear site.

For the calculation of the susceptibility χ_{P}, the Pauli expression [24] for non-interacting electrons was chosen,

$$\chi_{\text{P}} = \mu_{\text{B}}^2\, n(E) , \tag{23}$$

where μ_{B} is the Bohr magneton.

Equations (22), (23) and (14) yield a theoretical expression for K_{s} as a function of the s-part of the APW charge

$$K_{\text{s,th}}^{\text{d}} = \frac{8\pi}{3} \mu_{\text{B}}^2\, N(E_{\text{F}}) \langle Q_{\nu 0}^{\boldsymbol{k}} G_{\nu 0}^{\boldsymbol{k}} / I_{\nu 0}^{\boldsymbol{k}} \rangle_{\text{F}} . \tag{24}$$

Different regions of the Fermi surface give very different average electron densities at the nuclear position. Therefore, the evaluation of the mean value requires calculations at a large number of $\boldsymbol{k}$ points. The $\boldsymbol{k}$ states at the Fermi surface are given by the intersection points of the curves $E = E_{\text{F}}$ and $E = E(\boldsymbol{k})$ for different directions in $\boldsymbol{k}$ space. The curve $E = E(\boldsymbol{k})$ was constructed from the energy values given in Tables A1 and A2, respectively, using the boundary conditions for the shape of the energy bands. For the obtained $\boldsymbol{k}$ points at the Fermi surface, the energies, the APW charges, the values of $I_{\nu l}^{\boldsymbol{k}}$ and $G_{\nu l}^{\boldsymbol{k}}$ and the mean values of $Q_{\nu 0}^{\boldsymbol{k}} G_{\nu 0}^{\boldsymbol{k}} / I_{\nu 0}^{\boldsymbol{k}}$ were calculated. Table 2 shows an example of the $k_z = \pi/4a$ plane for two different Fermi energies. The calculated values $K_{\text{s,th}}^{\text{d}}$ are given in Table 3. The values of $K_{\text{s,th}}^{\text{d}}$ are about two or three times smaller than the observed Knight shift K_{s}.

Table 2. Electron states near the Fermi surface in the plane $k_z=\pi/4\,a$ of the $\boldsymbol{k}$ space for two different Fermi energies E_F. The electron states are described by the $\boldsymbol{k}$ vektor in units of $\pi/4\,a$, by the energy value (in Ry), and by the band index. The APW charges in the atomic spheres ν and outside the spheres are listed too. The Fermi contact terms for these states are given by $K_{\boldsymbol{k}}=2.235\times10^{-4}\,N(E_F)\,Q^{\boldsymbol{k}}_{\mathrm{Cd},0}\;G/I$ and the direct part of the Knight shift by the mean value of $K_{\boldsymbol{k}}$.
a) $E_F=0.368$ Ry and $N(E_F)=34$ electrons per unit cell and per Ry.
b) $E_F=0.348$ Ry and $N(E_F)=29$ electrons per unit cell and per Ry.

a

$\boldsymbol{k}$			energy (band)	ν	APW-charges $Q^{\boldsymbol{k}}_{\nu,0}$	$Q^{\boldsymbol{k}}_{\nu,1}$	$Q^{\boldsymbol{k}}_{\nu,2}$	$Q^{\boldsymbol{k}}_{\mathrm{out}}$	I [1]	G [1]	$K_{\boldsymbol{k}}\times10^2$
			0.3702	Ca	0.0110	0.0460	0.5773				
0.0	1.5	1.0	(2nd band)	Cd	0.0101	0.0720	0.0307	0.2502	1.972	35.24	0.137
			0.3718	Ca	0.0125	0.0532	0.5697				
1.0	1.6	1.0	(2nd band)	Cd	0.0047	0.0805	0.0287	0.2474	1.952	35.60	0.066
			0.3660	Ca	0.0479	0.0219	0.5362				
2.0	2.0	1.0	(2nd band)	Cd	0.0352	0.0997	0.0246	0.2278	2.000	34.82	0.468
			0.3691	Ca	0.0587	0.0219	0.4936				
2.0	2.0	1.0	(3rd band)	Cd	0.0157	0.1153	0.0220	0.2645	2.137	34.84	0.196
			0.3610	Ca	0.0097	0.1011	0.3424				
3.0	2.6	1.0	(3rd band)	Cd	0.0049	0.2117	0.0140	0.3095	2.006	34.42	0.064
			0.3703	Ca	0.0	0.0764	0.4080				
4.0	2.7	1.0	(3rd band)	Cd	0.0028	0.2105	0.0115	0.2830	2.055	35.28	0.037

b

$\boldsymbol{k}$			energy (band)	ν	APW-charges $Q^{\boldsymbol{k}}_{\nu,0}$	$Q^{\boldsymbol{k}}_{\nu,1}$	$Q^{\boldsymbol{k}}_{\nu,2}$	$Q^{\boldsymbol{k}}_{\mathrm{out}}$	I [1]	G [1]	$K_{\boldsymbol{k}}\times10^2$
			0.3519	Ca	0.0345	0.0634	0.4417				
0.0	1.9	1.0	(2nd band)	Cd	0.0304	0.1126	0.0283	0.2861	2.034	33.75	0.326
			0.3457	Ca	0.0423	0.0705	0.3827				
1.0	2.1	1.0	(2nd band)	Cd	0.0332	0.1345	0.0291	0.3037	1.844	33.28	0.388
			0.3459	Ca	0.0412	0.0648	0.4070				
2.0	0.2	1.0	(2nd band)	Cd	0.0326	0.1263	0.0292	0.2957	1.883	33.20	0.372
			0.3492	Ca	0.0543	0.0522	0.3967				
2.0	2.3	1.0	(2nd band)	Cd	0.0398	0.1442	0.0229	0.2839	1.969	33.35	0.436
			0.3481	Ca	0.0999	0.0481	0.2954				
3.0	3.0	1.0	(3rd band)	Cd	0.0001	0.1966	0.0144	0.3410	1.923	33.17	0.001
			0.3570	Ca	0.0023	0.1063	0.3020				
3.0	3.7	1.0	(3rd band)	Cd	0.0039	0.2423	0.0094	0.3258	1.946	34.31	0.045
			0.3491	Ca	0.0	0.1304	0.2388				
4.0	3.3	1.0	(3rd band)	Cd	0.0031	0.2654	0.0050	0.3490	1.936	33.45	0.035

[1] For the definition of I and G, see Eq. (11 c) and (21), respectively.

Table 3. Knight shift (experimental and theoretical), spin densities at the nuclear sites, and Pauli susceptibilities for CaCd and CaTl.

Alloy	CaCd	CaTl
Nucleus considered	^{113}Cd	^{205}Tl
Spin density at the nucleus considered	0.34 a.u.	0.44 a.u.
Spin susceptibility	2.03	1.3 c.g.s. volume units $\times 10^{-6}$
Knight shift at the nucleus considered	0.22×10^{-2} I 0.26×10^{-2} II	0.18×10^{-2} I 0.49×10^{-2} II
Measured Knight shift	0.38×10^{-2}	1.67×10^{-2}

I Without relativistic correction.
II Relativistic corrected values.

This was found by different authors doing Knight shift calculations [25–28]. In the approximation used here, the following important contributions to the total Knight shift were not included: a) The electron-electron interaction for the paramagnetic susceptibility [29, 30]; b) The relativistic effects and the modification given by a self-consistent APW method in the band structure calculation; c) The orbital effects; d) The different kinds of core polarisations [31], and e) The dependence of the Knight shift upon the chosen reference solutions as consequence of the chemical shift [32]. The difference between our theoretical results and the experimental data is prob-

ably due to the neglect of the terms mentioned above.

2. *Discussion of the* ^{113}*Cd-NMR in CaCd*

The direct Knight shift K_s^d depends on the spin density at the nuclei and the density of states at the Fermi energy. We shall discuss both terms separately and compare the calculated values with those of Cd metal.

For CaCd the Fermi energy lies in the energy range of the narrow d-like bands. These narrow bands cause a great density of states as is shown in Figure 6. We obtain 29 electrons per unit cell and per Ry for the density $N(E_F)$ at the Fermi energy, while the corresponding value given by the free electron theory is only 13 electrons per unit cell and Ry. There are no d-bands in Cd metal near the Fermi energy. The band structure calculation of Kasowski [27] shows that in Cd metal at the temperature of zero degree Kelvin, $N(E_F)$ is about 1.9 times smaller than the value given by the free electron model. Neither in this paper nor by Kasowski was the exchange enhancement factor for the susceptibility investigated. Jena et al. [26] calculated for this factor a value of 1.17 for Cd metal using the theory of Silverstein [29].

The calculated spin density at the Cd nuclei in CaCd, given in Table 3, is very small because the s part of the square of the wave function for states at the Fermi surface is small. As shown in Table 2, the APW charge $Q^{\boldsymbol{k}}_{\mathrm{Cd},0}$ for these states is small compared with $Q^{\boldsymbol{k}}_{\mathrm{out}}$, $Q^{\boldsymbol{k}}_{\mathrm{Cd},1}$, and $Q^{\boldsymbol{k}}_{\mathrm{Ca},2}$, especially for states of the third energy band. The quantity $\langle|\psi_{\boldsymbol{k}}(\boldsymbol{r}_\nu)|^2\rangle_F\,\Omega$ for CaCd is 130. In Cd metal, the spin density at the nuclear position is larger than in CaCd. Kasowski obtained 495 for $\langle|\psi_{\boldsymbol{k}}(\boldsymbol{r}_\nu)|^2\rangle_F\,\Omega$.

The polarisation and relativistic effects are not enclosed in the values for the spin density discussed above. Jena et al. determined for the polarisation part of the Knight shift in Cd metal 10% of the direct portion of K_s. Because the value for CaCd should be of the same order, the main correction to K_s^d is probably the relativistic one.

To determine the relativistic effects in a first approximation, not the absolute value for the spin density but only the relative change ξ of the density with reference to the free atom

$$\xi = \langle|\psi_{\boldsymbol{k}}(\boldsymbol{r}_\nu)|^2\rangle_F / |\psi_A(0)|^2 \qquad (25)$$

is taken from the APW calculation.

$|\psi_A(0)|^2$ is the electron density of an outer s electron of the atom. For K_s^d in Eq. (18), the absolute value of the spin density is transformed to the atomic hyperfine coupling constant of the s electron $a(s)$. K_s^d is then given by [23]

$$K_s^d = \chi_P\,\Omega\,\frac{1}{2\hbar\,\mu_B}\,\frac{I}{\mu_I}\,\xi\,a(s)\,. \qquad (26)$$

I is the nuclear spin and μ_I the magnetic moment of the nuclei. The problem is the choice of $a(s)$. For monovalent atoms $a(s)$ can be obtained from the results of atomic beam experiments. Values for polyvalent atoms can be derived from measurements on excited ionic states [23]. However, the value for Cd given by Knight is obviously too small [33]. For $a(s)$ we chose, therefore, the corrected Hartree-Fock-Slater values of Bennett et al. [12, 34]. These are calculated values for $a(s)$ or corrected densities of states according to the equation [23]

$$a(s) = \frac{16\,\pi}{3}\,\frac{\mu_I}{I}\,\hbar\,\mu_B\,|\psi_A(0)|_C^2\,. \qquad (27)$$

In the densities $|\psi_A(0)|_C^2$ core polarisation and relativistic effects are enclosed by multiplying the Hartree-Fock-Slater densities $|\psi_A(0)|^2_{HFS}$ with a scale factor. The corrected densities $|\psi_A(0)|_C^2$ for Cd and Tl are $13.3\,a_0^{-3}$ and $64.8\,a_0^{-3}$, respectively.

The Knight shift of Cd at the temperature of zero degree Kelvin is 0.34% [35]. Substituting the spin density and density of states calculated by Kasowski [27] into Eq. (18), it follows $K_s^d = 0.221\%$. This value is about a factor of 1.55 smaller than the experimental one. Considering the relativistic correction as described, the factor reduces to 1.3, which is in good agreement with the enhancement factor for the susceptibility given by Jena et al. [26] However, the density $|\psi_A(0)|^2_{HFS}$ is a function of the electron configuration and the atomic potential.

In this paper the atomic electron density is calculated using the program of Herman and Skillman [20]. The unmodified Hartree-Fock-Slater potential and the electron configuration of Table 1 were used and $|\psi_A(0)|^2_{HFS} = 11.175\,a_0^{-3}$ for Cd and $23.65\,a_0^{-3}$ for Tl was found. For CaCd the calculated ξ is 0.03. This is very small because the wave function of an atomic s electron has large portions of higher angular moments in the alloy and the states with larger s density are lying below the Fermi level. In Cd metal ξ amounts to 0.16. The corrected value for K_s^d in CaCd is 0.26%, which is about a factor of 1.4 smaller than the observed one.

For CaTl, the corrected spin density and the energy density at the Fermi energy are also calculated and given in Table 3, together with the calculated Knight shift. The value for $K^{d}_{s,th}$ is about a factor of 3.4 too small, although the relativistic correction is enclosed. As discussed below, in CaTl the relativistic effects cannot be taken into account by a simple correction factor.

3. *Discussion of the Cd-NMR in CaCd – CaTl*

Although it is not possible to verify the absolute value of the Knight shift, we assume that the shape of K_s in $CaCd_{1-x}Tl_x$ as a function of x is due to the variation of the direct part of the Knight shift. Starting with CaCd, the third partner in the alloy $CaCd_{1-x}Tl_x$ should not change the run of the electron bands. Only the position of the Fermi energy is shifting (rigid band model). The increase of the Tl concentration in $CaCd_{1-x}Tl_x$ increases the valence electron concentration VEC

$$\mathrm{VEC} = 2 + 0.5\,x\,. \tag{28}$$

The increase of x results in a shift of the Fermi energy which can be calculated using Eqs. (16) or (17). The change of the Fermi energy affects $K_s(x)$ twice. First, the density of states $N(E_F)$ changes, and second, the Fermi surface varies with x and therefore the spin density has to be averaged over other states.

K_s is also a function of the volume of the unit cell Ω. This volume effect can be neglected for the system $CaCd_{1-x}Tl_x$, because the maximum change of the lattice constants amounts to 0.4% [1].

In $CaCd_{1-x}Tl_x$ the Knight shift of the Cd-NMR has been measured in the range $0 \leqq x \leqq 0.5$. In the same range the VEC changes from 2 to 2.25 and the Fermi energy from 0.348 to 0.368 Ry. Figure 6 shows that the density of states $N(E)$ increases in this energy interval from 29 to 34 electrons per unit cell and per Ry, whereas $K_s(x)$ decreases from 0.38 to 0.31%. This decrease of K_s is due to the decrease of the s density at the Cd nuclei, which compensates the increase of the density of states. If the VEC varies from 2 to 2.25, mainly the d bands of Ca are filled, whereas the s and p density decrease.

In Table 2 the APW charges are listed for states near the Fermi surface for the two Fermi energies 0.348 Ry and 0.368 Ry, respectively. If the corresponding states of each band for the two Fermi energies are compared, the values for $Q^{k}_{Cd,0}$ are lowered for the higher Fermi energy. Table 2 shows also that there are great differences between the values of the APW charges for the second and third band. The s charge of Cd in the second band is about a factor ten larger than in the third band. It can be derived from Fig. 8 that the Fermi surface

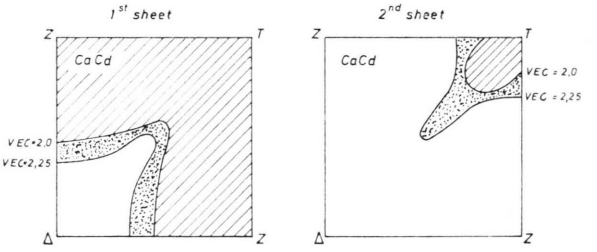

Fig. 8. First and second sheet of the Fermi surface for CaCd in the plane $k_z = \pi/4\,a$ of the Brillouin zone. Only a quarter of the surface is plotted. Δ, T, and Z are points of the Brillouin zone having the same symmetry as the corresponding points of Figure 3. The change of the Fermi surface with increasing valence electron concentration (VEC) is shown too.

of the second band (third band) decreases (increases) with increasing VEC. Therefore, the s density at the Cd nuclei decreases with increasing VEC. The results of the calculation of $K_s(x)$ are given in Figure 9. For CaCd the theoretical curve $K^{d}_{s,th} = f(x)$ has the same slope as the experimental curve $K_s = f(x)$. Also the s partial density of states of Cd

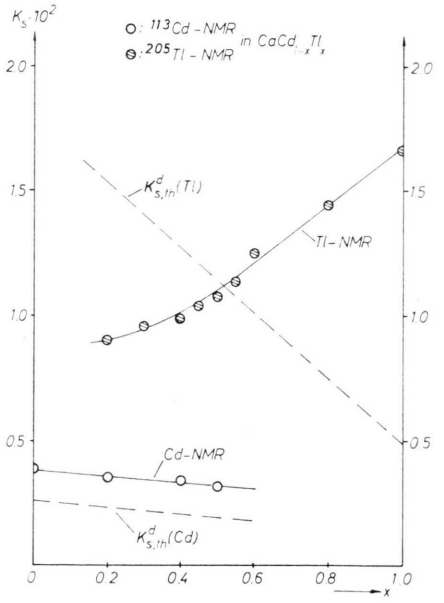

Fig. 9. Measured Knight shift K_s and calculated Knight shift $K^{d}_{s,th}$ of the ^{113}Cd- and the ^{205}Tl-NMR in the system $CaCd_{1-x}Tl_x$ as a function of x.

has the same shape as the function $K_{s,th}^{d}$. The change of K_s as a function of x is small in the region $0 \leqq x \leqq 0.5$, because the s partial density of Cd has a broad peak in the corresponding energy range of 0.35 Ry ($x=0$) and 0.37 Ry ($x=0.5$).

4. Discussion of the Tl-NMR

The Knight shift of the Tl-NMR in the quasi-binary $CaCd_{1-x}Tl_x$ has been calculated using the same method as for the Cd-NMR. Then the third partner in the intermetallic phases, Cd, reduces the VEC and consequently, the Fermi energy. Figure 9 shows the disagreement between the calculated and the measured values of the Knight shift. K_s of the Tl-NMR decreases with decreasing VEC, whereas the calculation yields an increasing Knight shift. The discrepancy between the experiments and the calculations is understandable, as a full relativistic APW (RAPW) calculation is necessary for CaTl [36]. It might be possible that in the RAPW calculation for CaTl the sequence of the energy bands is different from the sequence given by an APW calculation. Then the partial densities at the Fermi surface change their values essentially. This relative shift of the bands cannot be taken into account by a relativistic correction factor only. Therefore it is planned to do RAPW calculations for CaTl.

Acknowledgment

The authors acknowledge gratefully that part of the work was supported by the Deutsche Forschungsgemeinschaft.

[1] J. D. Marcoll, P. C. Schmidt, and A. Weiss, preceding paper.
[2] T. L. Loucks, Augmented Plane Wave Method, W. A. Benjamin, New York 1967.
[3] L. F. Mattheiss, J. H. Wood, and A. C. Switendick, A Procedure for Calculating Electronic Energy Bands Using Symmetrized Augmented Plane Waves, in: B. Alder (Ed.), Methods in Computational Physics, Vol. 8, Academic Press, New York 1968.
[4] E. A. Stern, Phys. Rev. **157**, 544 [1967].
[5] F. J. Arlinghaus, Phys. Rev. **157**, 491 [1967]; ibid. **186**, 609 [1969].
[6] K. H. Johnson and J. W. D. Connolly, Intern. J. of Quantum Chemistry **IIIS**, 813 [1970].
[7] S. J. Cho, Phys. Stat. Sol. **41**, 179 [1970].
[8] M. Belakhovsky, J. Pierre, and D. K. Ray, Phys. Rev. **B 6**, 939 [1972].
[9] C. H. Townes, C. Herring, and W. D. Knight, Phys. Rev. **77**, 852 [1950].
[10] S. D. Mahanti and T. P. Das, Phys. Rev. **183**, 674 [1969].
[11] L. Tterlikkis, S. D. Mahanti, and T. P. Das, Phys. Rev. **B 1**, 2041 [1970].
[12] L. H. Bennett, R. W. Mebs, and R. E. Watson, Phys. Rev. **171**, 611 [1968].
[13] R. E. Watson, L. H. Bennett, and A. J. Freeman, Phys. Rev. Letters **20**, 653 [1968]; ibid. **20**, 1221 [1968]; Phys. Rev. **179**, 590 [1969].
[14] J. Friedel, Phil. Mag. **43**, 153 [1952].
[15] A. Blandin and E. Daniel, J. Phys. Chem. Solids **10**, 126 [1959].
[16] L. C. R. Alfred and D. O. Van Ostenburg, Phys. Rev. **161**, 569 [1967]; Phys. Letters **26 A**, 27 [1967].
[17] J. C. Slater, Phys. Rev. **81**, 385 [1951].
[18] J. C. Slater, Phys. Rev. **51**, 846 [1937].
[19] V. Ern and A. C. Switendick, Phys. Rev. **137**, A 1927 [1965].
[20] F. Herman and S. Skillman, Atomic Structure Calculations, Eglewood Cliffs, New Jersey, Prentice Hall Inc. 1963.
[21] G. A. Burdick, Phys. Rev. **129**, 138 [1963].
[22] E. C. Snow and J. T. Waber, Phys. Rev. **157**, 570 [1967].
[23] W. D. Knight, Solid State Phys. **2**, 93 [1956].
[24] W. Pauli, Z. Physik **41**, 81 [1927].
[25] S. D. Mahanti and T. P. Das, Phys. Rev. **B 3**, 1599 [1971].
[26] P. Jena, T. P. Das, G. D. Gaspari, and S. D. Mahanti, Phys. Rev. **B 1**, 1160 [1970].
[27] R. V. Kasowski, Phys. Rev. **187**, 891 [1969].
[28] A. Gupta and S. Kumar, Nuclear Physics and Solid State Physics Symposium, Bombay, India, 1—4 Feb 1972.
[29] S. D. Silverstein, Phys. Rev. **130**, 912 [1963].
[30] T. Moriya, J. Phys. Soc. Japan **18**, 516 [1963].
[31] M. H. Cohen, D. A. Goodings, and V. Heine, Proc. Phys. Soc. London **73**, 811 [1959].
[32] M. Schlaak and A. Weiss, Sol. State Comm. **8**, 1241 [1970].
[33] T. J. Rowland and F. Borsa, Phys. Rev. **134**, A 743 [1964].
[34] L. H. Bennett, R. E. Watson, and G. C. Carter, J. Research National Bureau of Standards **74 A**, 569 [1970].
[35] R. V. Kasowski and L. M. Falicov, Phys. Rev. Letters **22**, 1001 [1969].
[36] H. Overhof and J. Treusch, Sol. State Comm. **9**, 53 [1971].